

Nonlinear optical frequency conversion of an amplified Fourier Domain Mode Locked (FDML) laser

Rainer Leonhardt^{1,2}, Benjamin R. Biedermann³, Wolfgang Wieser³ and Robert Huber^{3*}

¹Physics Dept, The University of Auckland, Private Bag 92019, Auckland, New Zealand

²Center for Integrated Protein Science Munich (CIPSM), Fakultät für Physik, Ludwig-Maximilians-Universität München, Oettingenstr. 67, 80538 Munich, Germany

³Lehrstuhl für BioMolekulare Optik, Fakultät für Physik, Ludwig-Maximilians-Universität München, Oettingenstr. 67, 80538 Munich, Germany

*Robert.Huber@LMU.DE

Abstract: We report on the highly efficient non-linear optical frequency conversion of the wavelength swept output from a Fourier Domain Mode Locked (FDML) laser. Different concepts for power scaling of FDML lasers by post-amplification with active fibers are presented. A two-stage post-amplification of an FDML laser with an amplification factor of 300 up to a peak power of 1.5 W is used to supply sufficient power levels for non-linear conversion. Using a single-mode dispersion shifted fiber (DSF), we convert this amplified output that covers the region between 1541 nm and 1545 nm to a wavelength range from 1572 nm to 1663 nm via modulation instability (MI). For this four wave mixing process we observe an efficiency of ~40%. The anti-Stokes signal between 1435 nm and 1516 nm was observed with lower conversion efficiency. In addition to shifting the wavelength, the effect of MI also enables a substantial increase in the wavelength sweep rate of the FDML laser by a factor of ~50 to 0.55 nm/ns.

©2009 Optical Society of America

OCIS codes: (190.4370) Nonlinear optics, fibers; (140.3600) Lasers, tunable; (060.2320) Fiber optics amplifiers and oscillators; (190.4380) Nonlinear optics, four-wave mixing; (230.7405) Wavelength conversion devices; (060.2410) Fibers, erbium.

References and links

1. R. Huber, M. Wojtkowski, and J. G. Fujimoto, "Fourier Domain Mode Locking (FDML): A new laser operating regime and applications for optical coherence tomography," *Opt. Express* **14**(8), 3225–3237 (2006), <http://www.opticsinfobase.org/oe/abstract.cfm?URI=oe-14-8-3225>.
2. M. Y. Jeon, J. Zhang, and Z. P. Chen, "Characterization of Fourier domain mode-locked wavelength swept laser for optical coherence tomography imaging," *Opt. Express* **16**(6), 3727–3737 (2008), <http://www.opticsinfobase.org/oe/abstract.cfm?URI=oe-16-6-3727>.
3. E. J. Jung, C. S. Kim, M. Y. Jeong, M. K. Kim, M. Y. Jeon, W. Jung, and Z. P. Chen, "Characterization of FBG sensor interrogation based on a FDML wavelength swept laser," *Opt. Express* **16**(21), 16552–16560 (2008), <http://www.opticsinfobase.org/oe/abstract.cfm?URI=oe-16-21-16552>.
4. Y. Wang, W. Liu, J. Fu, and D. Chen, "Quasi-distributed fiber Bragg grating sensor system based on a Fourier domain mode locking fiber laser," *Laser Phys.* **19**(3), 450–454 (2009), <http://www.springerlink.com/content/p300147134334266/>.
5. R. Huber, M. Wojtkowski, K. Taira, J. G. Fujimoto, and K. Hsu, "Amplified, frequency swept lasers for frequency domain reflectometry and OCT imaging: design and scaling principles," *Opt. Express* **13**(9), 3513–3528 (2005), <http://www.opticsinfobase.org/oe/abstract.cfm?URI=oe-13-9-3513>.
6. D. C. Adler, Y. Chen, R. Huber, J. Schmitt, J. Connolly, and J. G. Fujimoto, "Three-dimensional endomicroscopy using optical coherence tomography," *Nat. Photonics* **1**(12), 709–716 (2007), <http://www.nature.com/nphoton/journal/v1/n12/abs/nphoton.2007.228.html>.
7. D. C. Adler, S. W. Huang, R. Huber, and J. G. Fujimoto, "Photothermal detection of gold nanoparticles using phase-sensitive optical coherence tomography," *Opt. Express* **16**(7), 4376–4393 (2008), <http://www.opticsinfobase.org/oe/abstract.cfm?URI=oe-16-7-4376>.

8. P. M. Andrews, Y. Chen, M. L. Onozato, S. W. Huang, D. C. Adler, R. A. Huber, J. Jiang, S. E. Barry, A. E. Cable, and J. G. Fujimoto, "High-resolution optical coherence tomography imaging of the living kidney," *Lab. Invest.* **88**(4), 441–449 (2008), <http://www.nature.com/labinvest/journal/v88/n4/full/labinvest20084a.html>.
9. B. R. Biedermann, W. Wieser, C. M. Eigenwillig, G. Palte, D. C. Adler, V. J. Srinivasan, J. G. Fujimoto, and R. Huber, "Real time en face Fourier-domain optical coherence tomography with direct hardware frequency demodulation," *Opt. Lett.* **33**(21), 2556–2558 (2008), <http://www.opticsinfobase.org/ol/abstract.cfm?URI=ol-33-21-2556>.
10. C. M. Eigenwillig, B. R. Biedermann, G. Palte, and R. Huber, "K-space linear Fourier domain mode locked laser and applications for optical coherence tomography," *Opt. Express* **16**(12), 8916–8937 (2008), <http://www.opticsinfobase.org/oe/abstract.cfm?URI=oe-16-12-8916>.
11. C. M. Eigenwillig, W. Wieser, B. R. Biedermann, and R. Huber, "Subharmonic Fourier domain mode locking," *Opt. Lett.* **34**(6), 725–727 (2009), <http://www.opticsinfobase.org/ol/abstract.cfm?URI=ol-34-6-725>.
12. S. W. Huang, A. D. Aguirre, R. A. Huber, D. C. Adler, and J. G. Fujimoto, "Swept source optical coherence microscopy using a Fourier domain mode-locked laser," *Opt. Express* **15**(10), 6210–6217 (2007), <http://www.opticsinfobase.org/oe/abstract.cfm?URI=oe-15-10-6210>.
13. R. Huber, D. C. Adler, and J. G. Fujimoto, "Buffered Fourier domain mode locking: Unidirectional swept laser sources for optical coherence tomography imaging at 370,000 lines/s," *Opt. Lett.* **31**(20), 2975–2977 (2006), <http://www.opticsinfobase.org/ol/abstract.cfm?URI=ol-31-20-2975>.
14. R. Huber, D. C. Adler, V. J. Srinivasan, and J. G. Fujimoto, "Fourier domain mode locking at 1050 nm for ultra-high-speed optical coherence tomography of the human retina at 236,000 axial scans per second," *Opt. Lett.* **32**(14), 2049–2051 (2007), <http://www.opticsinfobase.org/ol/abstract.cfm?URI=ol-32-14-2049>.
15. M. W. Jenkins, D. C. Adler, M. Gargsha, R. Huber, F. Rothenberg, J. Belding, M. Watanabe, D. L. Wilson, J. G. Fujimoto, and A. M. Rollins, "Ultrahigh-speed optical coherence tomography imaging and visualization of the embryonic avian heart using a buffered Fourier Domain Mode Locked laser," *Opt. Express* **15**(10), 6251–6267 (2007), <http://www.opticsinfobase.org/oe/abstract.cfm?URI=oe-15-10-6251>.
16. T. Klein, W. Wieser, B. R. Biedermann, C. M. Eigenwillig, G. Palte, and R. Huber, "Raman-pumped Fourier-domain mode-locked laser: analysis of operation and application for optical coherence tomography," *Opt. Lett.* **33**(23), 2815–2817 (2008), <http://www.opticsinfobase.org/ol/abstract.cfm?URI=ol-33-23-2815>.
17. L. A. Kranendonk, X. An, A. W. Caswell, R. E. Herold, S. T. Sanders, R. Huber, J. G. Fujimoto, Y. Okura, and Y. Urata, "High speed engine gas thermometry by Fourier-domain mode-locked laser absorption spectroscopy," *Opt. Express* **15**(23), 15115–15128 (2007), <http://www.opticsinfobase.org/oe/abstract.cfm?URI=oe-15-23-15115>.
18. V. J. Srinivasan, D. C. Adler, Y. L. Chen, I. Gorczynska, R. Huber, J. S. Duker, J. S. Schuman, and J. G. Fujimoto, "Ultrahigh-speed optical coherence tomography for three-dimensional and en face imaging of the retina and optic nerve head," *Invest. Ophthalmol. Vis. Sci.* **49**(11), 5103–5110 (2008), <http://www.iovs.org/cgi/content/abstract/49/11/5103>.
19. B. R. Biedermann, W. Wieser, C. M. Eigenwillig, T. Klein, and R. Huber, "Dispersion, coherence and noise of Fourier domain mode locked lasers," *Opt. Express* **17**(12), 9947–9961 (2009), <http://www.opticsinfobase.org/oe/abstract.cfm?URI=oe-17-12-9947>.
20. D. C. Adler, R. Huber, and J. G. Fujimoto, "Phase-sensitive optical coherence tomography at up to 370,000 lines per second using buffered Fourier domain mode-locked lasers," *Opt. Lett.* **32**(6), 626–628 (2007), <http://www.opticsinfobase.org/ol/abstract.cfm?URI=ol-32-6-626>.
21. M. Y. Jeon, J. Zhang, Q. Wang, and Z. Chen, "High-speed and wide bandwidth Fourier domain mode-locked wavelength swept laser with multiple SOAs," *Opt. Express* **16**(4), 2547–2554 (2008), <http://www.opticsinfobase.org/oe/abstract.cfm?URI=oe-16-4-2547>.
22. Y. X. Mao, C. Fluerau, S. Sherif, and S. D. Chang, "High performance wavelength-swept laser with mode-locking technique for optical coherence tomography," *Opt. Commun.* **282**(1), 88–92 (2009), <http://dx.doi.org/10.1016/j.optcom.2008.09.059>.
23. G. Y. Liu, A. Mariampillai, B. A. Standish, N. R. Munce, X. J. Gu, and I. A. Vitkin, "High power wavelength linearly swept mode locked fiber laser for OCT imaging," *Opt. Express* **16**(18), 14095–14105 (2008), <http://www.opticsinfobase.org/oe/abstract.cfm?URI=oe-16-18-14095>.
24. J. D. Harvey, R. Leonhardt, S. Coen, G. K. L. Wong, J. C. Knight, W. J. Wadsworth, and P. S. J. Russell, "Scalar modulation instability in the normal dispersion regime by use of a photonic crystal fiber," *Opt. Lett.* **28**(22), 2225–2227 (2003), <http://www.opticsinfobase.org/ol/abstract.cfm?URI=ol-28-22-2225>.
25. M. E. Marhic, K. K. Y. Wong, and L. G. Kazovsky, "Wide-band tuning of the gain spectra of one-pump fiber optical parametric amplifiers," *IEEE J. Sel. Top. Quantum Electron.* **10**(5), 1133–1141 (2004), http://ieeexplore.ieee.org/xpl/freeabs_all.jsp?tp=&arnumber=1366387&isnumber=29921.
26. A. Y. H. Chen, G. K. L. Wong, S. G. Murdoch, R. Leonhardt, J. D. Harvey, J. C. Knight, W. J. Wadsworth, and P. S. J. Russell, "Widely tunable optical parametric generation in a photonic crystal fiber," *Opt. Lett.* **30**(7), 762–764 (2005), <http://www.opticsinfobase.org/ol/abstract.cfm?URI=ol-30-7-762>.
27. A. S. Y. Hsieh, G. K. L. Wong, S. G. Murdoch, S. Coen, F. Vanholsbeeck, R. Leonhardt, and J. D. Harvey, "Combined effect of Raman and parametric gain on single-pump parametric amplifiers," *Opt. Express* **15**(13), 8104–8114 (2007), <http://www.opticsinfobase.org/oe/abstract.cfm?URI=oe-15-13-8104>.

28. J. S. Y. Chen, S. G. Murdoch, R. Leonhardt, and J. D. Harvey, "Effect of dispersion fluctuations on widely tunable optical parametric amplification in photonic crystal fibers," *Opt. Express* **14**(20), 9491–9501 (2006), <http://www.opticsinfobase.org/oe/abstract.cfm?URI=oe-14-20-9491>.
 29. G. K. L. Wong, A. Y. H. Chen, S. G. Murdoch, R. Leonhardt, J. D. Harvey, N. Y. Joly, J. C. Knight, W. J. Wadsworth, and P. S. Russell, "Continuous-wave tunable optical parametric generation in a photonic-crystal fiber," *J. Opt. Soc. Am. B* **22**(11), 2505–2511 (2005), <http://www.opticsinfobase.org/abstract.cfm?URI=josab-22-11-2505>.
 30. C. Jirauschek, C. Eigenwillig, B. Biedermann, and R. Huber, "Fourier Domain Mode Locking Theory," in *Conference on Lasers and Electro-Optics/Quantum Electronics and Laser Science Conference (IEEE, 2008)*, 1403–1404, <http://www.opticsinfobase.org/abstract.cfm?uri=CLEO-2008-CTuFF2>.
-

1. Introduction

Recently, the introduction of Fourier Domain Mode Locking (FDML) [1–4] has helped to overcome physical limitations of the sweep repetition rate of rapidly wavelength swept laser sources [5]. FDML lasers have proven superior performance in a series of biomedical imaging, spectroscopy and sensing applications [1,3,6–18]. In FDML a tunable optical bandpass filter is driven in resonance to the optical roundtrip time of light in a several kilometer long laser cavity. Still, up to now the FDML laser operates only around certain central wavelengths, determined by the availability of the different gain media, i.e. 1060 nm [14,18], 1300 nm [1,13], and 1550 nm [16,19] and their wavelength sweep rate is limited by the mechanical response of the tunable optical bandpass filter, which typically is either a Fiber Fabry-Perot Tunable Filter (FFP-TF) [1,20,21] or a grating based scanner with a rotating polygon mirror [22,23].

Up to 100 nm sweep range within 2.5 μ s have been demonstrated [13]. One method to overcome limitations in the accessible wavelength range and maximum sweep rate, given by the gain medium and the applied filter, is to utilize non-linear optical effects and frequency conversion. In this paper we will demonstrate a 40% efficient wavelength shift of up to ~125 nm with a 50-fold increase in wavelength sweep rate. As the average output power (and therefore the peak power) of an FDML laser is quite low (~mW), the output of the laser has to be amplified to the watt level before non-linear effects can be observed. In this paper we utilize the effect of Modulation Instability (MI), i.e. a four wave mixing process with degenerate pump, in the normal dispersion regime close to the zero-dispersion wavelength (ZDW) of a single-mode fiber [24–26]. As our FDML laser operates around 1547 nm, we used a dispersion-shifted fiber (DSF) with a ZDW of about 1545 nm for our experiments. In this paper we show that a small shift of the pump wavelength results in a large shift for the MI sidebands, therefore increasing the sweep rate considerable and shifting the FDML spectrum to another wavelength region.

2. Experimental setup and results

2.1 Experimental setup

Figure 1 shows the experimental setup with an FDML laser as primary light source. A detailed description of the FDML laser can be found elsewhere [19]. Here, we operate it at a central wavelength of 1547 nm and a scanning width of the filter of 100 nm. The sinusoidal driving signal is at 56.3 kHz and the output power is 5 mW. A booster semiconductor optical amplifier (BOA) acts as the first amplifier.

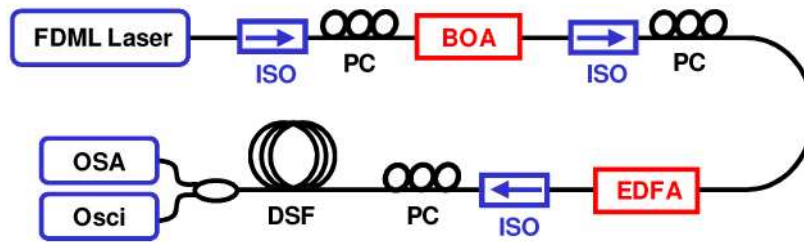


Fig. 1. Schematic diagram of the experimental setup: Light from the FDML laser is first amplified by the booster optical amplifier (BOA), and then by the erbium-doped fiber amplifier (EDFA). The nonlinear effects are generated in the dispersion-shifted fiber (DSF), and detected with the optical spectrum analyzer (OSA) and an oscilloscope (Osci).

The current of the amplifier can be modulated such that only a small fraction of the 100 nm sweep is amplified or, similar to a pulse picker, that only each n th sweep is amplified. An erbium-doped fiber amplifier (EDFA) is used as the second stage of the amplification process. A length of dispersion-shifted fiber (DSF) is employed as nonlinear medium. Polarization controllers (PC) are used to optimize the performance of the different elements, and the optical isolators (ISO) suppress spurious reflections and prevent catastrophic optical damage by back reflection. Two channels of an arbitrary waveform generator are used to provide the drive signal for the FDML laser, and to modulate the BOA synchronously. The outputs of the EDFA and the DSF are measured with an optical spectrum analyzer (OSA) and an oscilloscope (Osci).

2.2 Amplification: power scaling with erbium doped fiber amplifier (EDFA)

In order to achieve high instantaneous output power, an EDFA was chosen as second amplification stage. With a carrier lifetime of several 10 ms, much longer than the sweep repetition time of the FDML laser, for low duty cycles the instantaneous output power can be much higher than the average power. The concept now was to modulate the output of the FDML laser such that it is switched on for only a very short time. As shown in Fig. 2, there are two approaches to realize low duty cycles for high peak powers: (a) amplifying only a very small range of each sweep, reducing the wavelength sweep range at constant repetition rate (referred to as mode A) or (b) reducing the sweep repetition rate, like in a pulse picker scheme, but keeping the same sweep range (referred to as mode B).

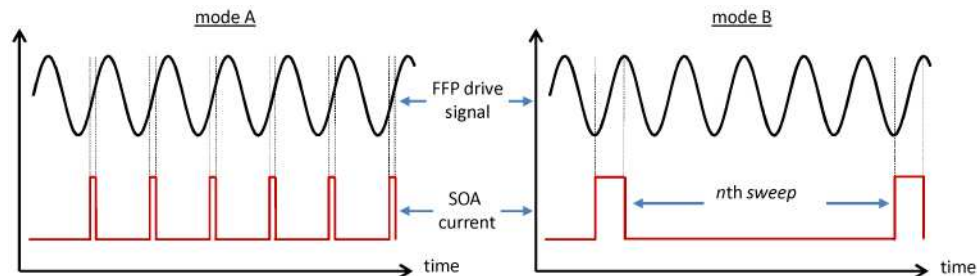


Fig. 2. Two modes of post amplification to increase the FDML power output. Mode A: Modulation at full repetition rate. Mode B: Modulation at reduced repetition rate.

2.2.1 Mode A: constant repetition rate / reduced sweep range

The BOA is modulated at the same frequency as the FDML laser. It is switched on for 180 ns within each 18 μ s full bidirectional sweep cycle of the laser, resulting in a duty cycle of only 1%, i.e. it amplifies 2% of one sweep direction of the sinusoidal wavelength sweep (1540.6 nm to 1544.8 nm). The 2% are the most linear part of the sweep close to the center. We chose these parameters for several reasons: a) the amplified wavelength range lies within the high

gain region for Modulation Instability (MI) for the DSF, b) a duty cycle of only 1% ensures high amplification in the EDFA, c) we can choose only the linear part of the frequency sweep of the FDML laser, and d) the repetition rate is kept at its original frequency of 56.3 kHz. The BOA amplifies the peak power of this small part of the spectrum by a factor of 15, therefore the peak power after the BOA is 75 mW. The remainder of the wavelength sweep is attenuated by the BOA with an extinction ratio of more than 30 dB. The EDFA consists of 6m of MetroGain fiber (Fibercore Ltd.) and is pumped in reverse direction by a 980 nm laser diode with a pump power of 250 mW. The optimum length of the EDF for our application was found by the cut-back method. Due to the short duty cycle, the EDFA amplifies the output of the BOA to a peak power of 1.5 W but also generates some background, mainly due to amplification of ASE generated by the BOA.

However, this background occurs only during 1% of the duty cycle, i.e. the background in between the amplified wavelength sweeps is negligible. Fig. 3 (left) shows the output after the BOA (trace A, red) and after the EDFA just before the DSF (trace B, blue). The average power after the EDFA was 34 mW, with about 15 mW contained in the desired spectral range (1540.6 nm to 1544.8 nm), and the rest in the very broad background. Fig. 3 (right) shows the output after the DSF for 0.15 W and 1.5 W injected peak power, respectively.

2.2.2 Mode B: constant sweep range / reduced sweep rate

We also tried to amplify the whole 100 nm wavelength sweep from the FDML output, i.e. operating the BOA with a duty cycle of 50%, but with a lower repetition rate. Due to the structure of the gain spectrum of the EDFA, the amplification was strongly modulated across the whole range (1497 nm to 1597 nm) with a peak power of about 0.1 W at the gain maximum at 1555 nm. To increase the peak power we used lower duty cycles by amplifying only 50% of every n th wavelength sweep (see Fig. 2). For $n=10$ the peak power at the gain maximum reached 0.6 W, while for even larger n the increase in peak power was less than 10%. Because the energy of each sweep is already in the μ J level, we attribute this saturation behavior to the limited number of laser active doping sites in the EDF available for amplification.

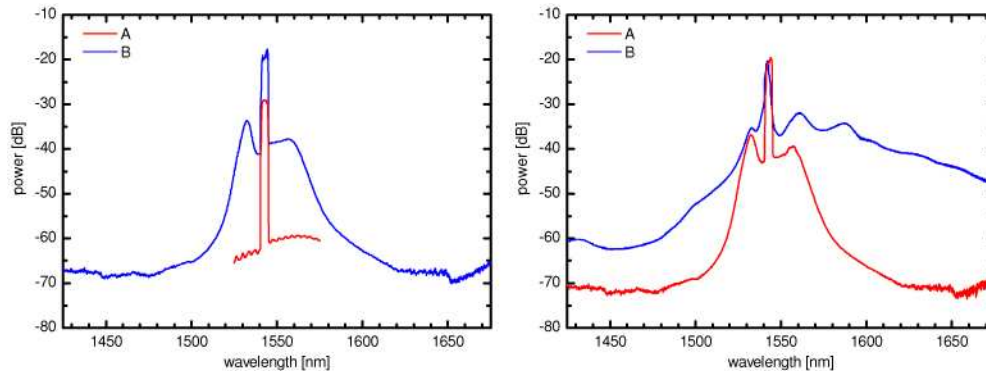


Fig. 3. Left: Output spectra of the laser after the BOA (red) and the EDFA (blue). Right: Spectra after DSF with lower power (red) and high power (blue). The spectral difference reflects the converted energy, as MI only occurs with sufficient peak power.

2.3 Nonlinear optical conversion: modulation instability (MI)

To observe nonlinear effects with the amplified sweeps from the FDML laser, we employed the effect of MI in the normal dispersion regime. For this type of four-wave-mixing (FWM), pump photons at frequency ω are converted into two sidebands, one at frequency $\omega_s = \omega - \Omega$ and one at frequency $\omega_a = \omega + \Omega$. The frequency shift Ω is determined by the dispersion characteristics of the fiber. Using the expansion coefficients β for the different orders of

dispersion, in the normal dispersion regime ($\beta_2 > 0$) MI can only occur close to the ZDW if $\beta_4 < 0$ [24]. The gain for the MI process also depends on Ω , as it is determined by the subtle interplay between the Kerr nonlinearity and the Raman effect [27].

2.3.1 Nonlinear optical conversion of stationary output

The DSF used for our experiments was obtained from Fujikura (JFS-00094A), had a ZDW of about 1545 nm, and an attenuation of 0.28 dB/km. We started with a length of 8.4 km, and by cutting off 2.05 km we saw no noticeable decrease in the overall gain of the fiber. On the other hand, by using the 2.05 km piece of the fiber, the nonlinear effects were barely noticeable. Therefore all results presented in this paper were recorded with the 6.35 km piece of DSF. To record the output spectra with an optical spectrum analyzer, the output of the DSF was appropriately attenuated.

Figure 4 shows the spectra for six fixed wavelength λ_p of the FDML laser (i.e. the laser was not operated as a swept source), namely $\lambda_p = 1540.8$ nm, 1542.0 nm, 1543.0 nm, 1543.7 nm, 1544.2 nm, and 1544.8 nm, respectively. It can be clearly seen that the Stokes sidebands generated by MI appear between $\lambda_s = 1663.1$ nm and 1572.2 nm, respectively (i.e. the shortest pump wavelength produces the sideband with the longest wavelength). The sidebands are up to 35 dB above the background, and the conversion efficiency into the Stokes sidebands is as high as 40% at $\lambda_p = 1544.2$ nm (light blue) but already reduced to 20% at $\lambda_p = 1543.7$ nm (dark blue). Weaker peaks are also visible on the Anti-Stokes side of the pump, and the smaller intensity can be explained by the large Raman gain for the Stokes sidebands [27]. The Raman gain is also responsible for the broad shoulder that appears at ~ 1650 nm for the long-wavelength Stokes sidebands. While the sidebands might not appear symmetric to the pump on a wavelength scale especially for weak peaks on a broad shoulder, the frequency shift due to the MI process is always symmetric about the pump frequency.

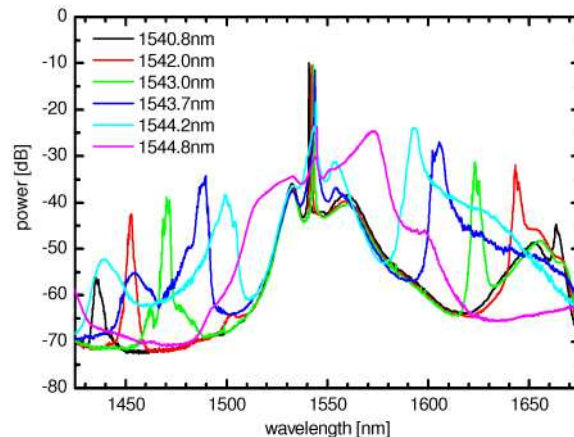


Fig. 4. Output spectra of the DSF for several fixed pump wavelengths. The longest-wavelength Stokes peak results from the shortest pump wavelength.

We also measured the static linewidth of the Stokes sidebands. Close to the edges of our tuning range, the linewidth increases due to the small gain but for most of the range the linewidth of the Stokes sideband lies between 1 nm for large detunings and 4 nm for small detunings. This trend is consistent with the theory [28], but our experimental values are larger than those predicted (~ 1 nm for small detunings). This discrepancy can be readily explained by considering small fluctuations of the core diameter that lead to a shift of the sideband detuning, and therefore to a larger bandwidth for a long fiber [29], which in our case had a length of 6.35 km.

2.3.2 Nonlinear optical conversion of wavelength swept FDML laser output

To investigate the conversion of the wavelength-swept output of the FDML laser, and distinguish MI effects from ASE background and other parasitic effects, the amplified output of the swept FDML laser covering the region between 1540.6 nm and 1544.8 nm (1% duty cycle, mode A) was used.

Figure 3 (right) shows the spectrum after the DSF when only 10% of the EDFA output is coupled into the DSF (trace A, red), while trace B (blue) shows the spectrum after the DSF with 100% coupled in but attenuated by a factor of 10 after the DSF before it enters the OSA. For trace A the peak power in the DSF is so low that no nonlinear effects are observed. Therefore by directly comparing trace A and trace B in Fig. 3 (right), it is evident that the nonlinear effect of MI has efficiently converted the pump light to a spectral range from 1550 nm to more than 1670 nm. While for trace A the pump wavelength region contains more than 90% of the total energy, in trace B about 45% of the total energy lie in the wavelength range of just the Stokes sideband. This indicates a conversion efficiency of ~40%. The gain for most Stokes wavelengths was about 25 dB while the gain for the Anti-Stokes wavelengths was only in the order of 10 dB. It can also be seen in Fig. 3 (right) that the gain for the Stokes sideband shows some modulation. To improve the flatness of the gain curve, the BOA could be driven with a time dependent (and therefore frequency dependent) signal that compensates for the frequency dependent gain of the MI process, similar to the concept demonstrated in [9].

We did not determine the dynamic bandwidth of the Stokes sidebands for the wavelength-swept case, because, due to the high sweep speed, it is difficult to directly measure the instantaneous linewidth in this case. But there is no indication that the instantaneous linewidth in the swept case should be different from the linewidth in the stationary case as discussed in section 2.3.1.

These results imply that an efficient conversion of the FDML wavelength sweep is possible. While the laser sweeps from 1540 nm to 1544 nm, an output sweeping from 1550 nm to 1675 nm is generated. This is the first demonstration of non-linear optical frequency conversion of the output of an FDML laser. Compared to an average sweep rate of just 0.011 nm/ns of the FDML laser, the wavelength sweep rate of the Stokes MI line has increased 50-fold to 0.55 nm/ns, i.e. ~100 nm in 180 ns.

3. Conclusion and outlook

In this paper we demonstrate for the first time non-linear optical frequency conversion of the rapidly wavelength swept output of an FDML laser. Two key features of the observed wavelength conversion are of general importance for FDML technology: (a) the wavelength shift makes spectral regions accessible which cannot be realized directly with the available gain media, (b) the non-linear wavelength response of the MI sidebands can provide an increase in sweep rate; in our case 50-fold.

The observed process showed a conversion efficiency of ~40% at the Stokes sideband, generating wavelength sweeps from ~1570 nm to ~1670 nm within 180 ns. The rate of 0.55 nm/ns represents the fastest wavelength sweep rate generated with an FDML laser to date. The required output power for pumping the MI process was realized by a fiber post-amplification stage. Different strategies to achieve high peak power from FDML lasers with rare earth doped fibers are demonstrated and discussed. The peak output power of 1.5 W represents the highest output power generated with FDML lasers to date.

Compared to the sinusoidal frequency sweep of the FDML laser itself, the frequency sweep generated by the MI process for mode A is much more linear. Furthermore, the nonlinearity in the sweep rate due to the nonlinear frequency shift generated by the MI process can be compensated by driving the filter of the FDML laser non sinusoidally, similar to the concept presented in [10].

By utilizing high-power EDFAs it should also be possible to obtain these nonlinear effects in continuous-wave experiments, e.g. scanning the FDML laser with the same repetition rate but only over the region from 1540 nm to 1544 nm. Several stages of EDFAs might be necessary to avoid backwards propagating ASE.

In the future, there are several potential applications of the demonstrated setup. A shift towards longer wavelengths could be used to perform optical coherence tomography in biological tissue around 1670 nm. Due to the local absorption minimum of water at this wavelength, a better penetration might be achieved. The increased sweep rate in combination with external optical buffering [13,14] might pave the road for ultra high speed OCT systems. Since a ~ 100 nm wavelength sweep within 180 ns was observed, theoretically a wavelength swept light source with a 5.5 MHz sweep repetition rate could be realized. Furthermore, as the presented sweep rate (or equivalently: the chirp of the output waveform) is high enough, an efficient temporal compression with a dispersion compensating fiber might be envisioned for the generation of high power ps or fs pulses; even though the wavelength-shifted light will not be fully coherent, due to the partial coherence of the FDML laser [16,30] and the relationship between the phases of the pump and the sidebands for the MI process, the wavelength-shifted light will also be partially coherent, therefore potentially allowing compression.

Acknowledgment

We would like to acknowledge the generous support from Prof. W. Zinth at the Ludwig-Maximilians-University Munich. This research was sponsored by the Emmy Noether program of the German Research Foundation (DFG – HU 1006/2-1) and the European Union project FUN-OCT (FP7 HEALTH, contract no. 201880). R. Leonhardt is a visiting Professor and was partially supported by the DFG-Cluster of Excellence Munich-Centre for Advanced Photonics.